INTERNATIONAL JOURNAL OF INTEGRATED ENGINEERING
ISSN: 2229-838X e-ISSN: 2600-7916

IJIE

Vol. 16 No. 1 (2024) 64-71
https://publisher.uthm.edu.my/ojs/index.php/ijie

Investigation into the Impact of Groove Shape on the Tensile Strength of Commercial Steel

Saleh Suliman Saleh Elfallah[1]*

[1] *College of Mechanical Engineering Technology, Benghazi, 00000, LIBYA*

*Corresponding Author: sselfallah87@gmail.com
DOI: https://doi.org/10.30880/ijie.2024.16.01.006

Article Info

Received: 24 October 2023
Accepted: 19 February 2024
Available online: 25 April 2024

Keywords

Commercial steel, GMAW, groove shape, mechanical properties, Taguchi method

Abstract

In the industrial landscape, welding holds a prominent position, with a significant demand for both effective and high-quality welding processes. Manufacturers, striving to maintain competitiveness, rely on their manufacturing engineers and production personnel to swiftly and efficiently establish manufacturing processes for new products. Among the various welding methods employed, Gas Metal Arc Welding (GMAW) stands out as one of the most widely utilized processes. Several input factors, including welding current, welding voltage, gas flow rate, wire feed speed (WFS), wire size, and welding speed, play a crucial role in determining the quality of welding outcomes. Taguchi's design, recognized for its effectiveness, serves as a powerful optimization tool for enhancing the quality and performance output of manufacturing processes. In this particular study, GMAW was employed to weld commercial steel under predetermined factors of welding voltage, WFS, and groove shape. The X-groove welding exhibited lower tensile strength and hardness compared to V-groove weldments. Utilizing Taguchi's design, the objective was to identify the optimal process factors that would result in higher tensile strength and hardness. The analysis revealed that welding groove shape had the most significant impact on both tensile strength and hardness, followed by voltage. In contrast, WFS exerted the least influence on tensile strength and hardness. The optimized combination of welding factors identified was a V-groove shape, 20 V welding voltage, and a 5.9 m/min WFS.

1. Introduction

Welding stands as an integral fabrication process in industries, both large and small, serving as a primary method for joining metals and facilitating repairs. This efficient, economical, and reliable process finds applications in various environments, including air, underwater, and even space. Gas Metal Arc Welding (GMAW) is extensively employed for welding both ferrous and non-ferrous metals. The choice of shielding gas, whether inert (e.g., argon or helium) or active (e.g., carbon dioxide and oxygen), plays a crucial role in protecting the molten weld pool. GMAW is versatile, applicable to a range of materials such as carbon steel, stainless steel, alloy steel, and aluminum. Metal transfer in GMAW occurs through different modes, including short-circuit, globular, spray, or pulsed. The quality of the resulting weld bead is influenced by factors such as welding current, arc voltage, electrode composition and size, welding travel speed, and the flow and gradient of the shielding gas. GMAW is capable of performing various joint types, including butt joints, corner joints, edge joints, lap joints, and T-joints. Overall, its adaptability and effectiveness make it a widely utilized welding process in the manufacturing and repair activities of diverse industries [1], [2], [3], [4].

The Taguchi method, introduced by Dr. Genichi Taguchi, presents a design approach known as an orthogonal array. This method enables the study of a greater number of factors or factor spaces with fewer experiments compared to the factorial design of experiments [5]. Despite its simplicity, the Taguchi Method is gaining increasing popularity in manufacturing industries, demonstrating its effectiveness and efficiency [6].

Numerous researchers have employed the Taguchi method to identify the optimal Gas Metal Arc Welding (GMAW) process factors for achieving higher tensile strength and hardness in mild steel [7], [8], [9], [10]. A study by Rajakumar et al. [7] showed that lower welding current and welding speed yielded maximum tensile strength on joining SAE 1022, low-carbon manganese steel using consumable electrode ER70S-6 copper-coated wire and a mixed shield gas of argon (Ar) and carbon dioxide (CO2) and a hardness value of 250 HV (≈100 HRB) at the fusion zone (FZ). Rout et al. [8] investigated the effect of welding parameters on the welding of AISI 1030 by ER70S-6 as an electrode wire and a mixture of shielding gas of 80% Ar and 20% CO2 and found that optimal tensile strength and FZ hardness were shown at higher welding voltage and current and at lower wire feed speed (WFS). The analysis was made based on L27 Taguchi's orthogonal array. However, Math and Kumar [9] studied the effect of welding voltage, current, and WFS on the welding of IS 2062 E250A mild steel and analyzed it based on an L9 orthogonal array. The results concluded that higher tensile strength and FZ hardness were shown at lower welding current, voltage, and WFS. Also, the WFS had the most influence on the tensile strength, followed by the welding current, while the welding voltage had a higher effect on the FZ hardness. Elfallah [10] concluded in a previous study that welding voltage had a higher influence on the FZ tensile strength and WFS on the FZ hardness. Also, lower voltage and WFS have contributed to the increased welding tensile strength and FZ hardness. These collective findings contribute to a comprehensive understanding of the factors influencing the mechanical properties of mild steel welds.

Studies have consistently observed that welding with higher tensile strength also exhibits higher FZ hardness [9, 10]. However, Sankar et al. [13] concluded the opposite. Additionally, the hardness of the base metal was reported, and it was found that the base metal has lower hardness than FZ [11], [12], and lower tensile strength but higher toughness [13]. The elevated current or voltage [10], [14], and WFS [15] result in higher heat input into the welding, inducing additional internal stresses in both the FZ and Heat-Affected Zone (HAZ), and widening the HAZ [16]. This, in turn, affects the mechanical properties within these regions [10], [14], [16], and [17]. The variation in tensile strength and hardness is mainly due to the microstructural changes in the FZ and HAZ that witness different grain sizes due to different heat inputs [10], [17]. The underlying cause of the lower tensile strength and hardness is associated with the grain structure, which appears coarse and dendritic in the FZ [3], [10], and [13].

This study discussed the effect of the welding parameters on the hardness and transverse tensile strength of mild steel welding. Mild steel is the most utilized steel in industry in Benghazi, Libya. The optimization of welding parameters for such materials is crucial for quality welding products. The welding parameters—welding voltage, WFS, and groove shape—were selected in this study. The effect of the groove shape parameter was included because such welding structures use different welding groove configurations. The analysis and optimization are based on the Taguchi Method.

2. Methodology

2.1 Materials and Experimentation

Mild steel was procured from the local market and underwent preparation at the Tasamim workshop in Benghazi using a CNC laser cutter. Sample preparation followed the guidelines outlined by the American Society of Testing Materials (ASTM) E8/E8M for the tensile test [18]. Fig. 1 illustrates the sample dimensions for the tensile test, featuring a fixed thickness of 10 mm and V and X groove shapes with angles set at 60° on each side. Welding in the X groove shape occurred on both sides, while in the V-groove shape, it was performed on a single side. These dimensions and configurations were established to adhere to the specified testing standards and ensure accurate and reliable tensile test results. The groove preparation of the samples was carried out at the College of Mechanical Engineering Technology. Additionally, other samples were readied for hardness testing and microstructure inspection.

The welding of the samples took place at the Saad Elkarimi Institute of Technology in Benghazi. Nexus copper-coated mild steel for GMAW served as the welding wire, and the welding machine employed was the CEA MAXI 321, as depicted in Fig. 2(a). The welding process itself is depicted in Fig. 2(b). A shielding gas combination of 82% argon and 18% carbon dioxide was utilized, with a gas flow rate of 18 milliliters per minute (ml/min). Table 1 provides the composition details of the joint metal and welding filler. The base metal adheres to the non-alloy structural steel specifications of the European standard EN 10025-2, specifically grade S235JR (1.0038), with AWS ER70 S-6 welding wire utilized as the welding filler. Table 2 presents the tensile strength and hardness values for both the base metal and welding filler.

Int. Journal of Integrated Engineering Vol. 16 No. 1 (2024) p. 64-71

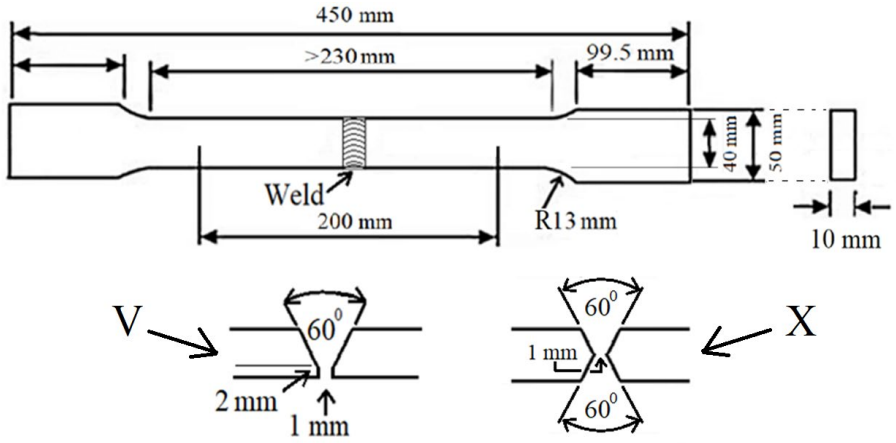

Fig. 1 *The dimensions of the samples for the tensile test were prepared in accordance with the guidelines outlined in ASTM E8/E8M [18], featuring both V and X groove shapes*

Table 1 *The metal joint and welding wire mineral compositions [19]*

Component	Composition							
	Cu	Mn	Cr	P	S	Ni	C	Fe
Base metal	0.55%	1.4%	-	0.025%	0.025%	0.012%	0.17%	Balanced
Welding filler	0.35%	1.8%	0.15%	0.035%	0.035%	0.15%	0.12%	Balanced

(a) **(b)**

Fig. 2 *Welding process (a) Welding machine; (b) Welding sample and GMAW nozzle*

Table 2 *The tensile strength and hardness of base metal and filler wire [19], [20]*

Component	Tensile properties			Hardness properties	
	Tensile strength	Yield strength	Elongation	Brinell hardness	Rockwell hardness B
Base metal	360-510	235	26%	≤120 HBW	66.7 HRB
Welding filler	583 MPa (81 ksi)	483 MPa (70 ksi)	24%	-	-

2.2 Taguchi's Design

The experimental design adheres to a 2-level, four-factor layout, yielding a total of 8 runs, a methodology commonly referred to as Taguchi's L8 array. The coded design values for the experiment are presented in Table 3, while Table 4 provides the corresponding actual values obtained during the experimental process. The analysis of the data was conducted using Minitab 18® to derive meaningful insights from the experimental results. A tensile test was performed using the Shimadzu (UEH-20) universal testing machine at the Libyan Iron and Steel Company in Misrata. The sample subjected to the tensile test is illustrated in Fig. 3(a). Additionally, a hardness test was conducted at the College of Mechanical and Engineering Technology in Benghazi, utilizing the Ernst Rockwell bench hardness tester, as depicted in Fig. 3(b). For the hardness test, a diamond cone indenter

with a load of 100 kg applied as a pressure force was employed. This methodology was employed to measure the hardness of the weld area, providing insights into the variations influenced by different welding factors.

Table 3 *Experimentation orthogonal array coding design*

Std order	A	B	C
1	1	1	1
2	1	1	2
3	1	2	1
4	1	2	2
5	2	1	1
6	2	1	2
7	2	2	1
8	2	2	2

Table 4 *Orthogonal array actual values with respect to welding factors*

Standard order	Voltage (v)	WFS (m/min)	Groove shape
1	20	5.9	V
2	20	5.9	X
3	20	10.6	V
4	20	10.6	X
5	27.5	5.9	V
6	27.5	5.9	X
7	27.5	10.6	V
8	27.5	10.6	X

3. Results and Discussion

Table 5 presents the Taguchi design layout, outlining the relationships between welding factors and the corresponding tensile strength and hardness of the weld samples. The heat input (HI) (KJ/mm) calculation is based on the general equation (Equation 1), taking into account that the thermal efficiency of GMAW is 0.8 [21]. The welding current, or amperage, is estimated to be 120 A at 20 V and 270 A at 27.5 V, while the welding speed is 150 mm/min.

$$HI = 0.8 \times \frac{Voltage(V) \times Amperage(A)}{Travelspeed(mm/\min) \times 1000} \quad (1)$$

The results indicate a direct correlation between hardness and tensile strength; as the hardness of FZ increased, the tensile strength increased, and vice versa. Furthermore, both tensile strength and hardness exhibited a decline with an increase in welding voltage and wire feed speed. Additionally, a consistent decrease in tensile strength and hardness was observed when the groove shape changed from V to X under the same voltage and wire feed speed conditions. However, an exception was noted at 20 V and 10.6 m/min, where the tensile strength and hardness of welding increased when the groove shape changed from V to X.

The decrease in tensile strength of the samples is noticed to be related to the decreased FZ hardness. Furthermore, it is related to the welding heat input increase as seen in Table 5. Moreover, the V-groove welding exhibited higher FZ hardness and tested tensile strength than X groove shaped welding at the same welding voltage and WFS. It could be related to that V-groove welding samples were exposed to three welding passes each to fill the opening gap comparing to two passes for X groove shaped welding. Each pass for each side for the double-sided groove. In other word, V-groove shape welding is exposed to increased heat input due to the accumulative heat each pass adds to the welding resulting in higher internal stresses. It's due to the increase of these stresses the FZ hardness get lower and resulting in lower samples tensile strength.

The increased heat was reported to increase the welding cooling rates [22], consequently leads to increased internal stresses and residual strains of welding. A study by Lahtinen et al. [23] showed that higher heat input

Int. Journal of Integrated Engineering Vol. 16 No. 1 (2024) p. 64-71

results in earlier localization of the strain and consequently lowers maximum strength. Ahmed et al. [24] also agree that heat input of welding affects its mechanical properties. Besides, the variation on welding hardness with the base metal could have led to the failure at FZ due to tensile test as seen in Fig. 3(a). Since the FZ has lower hardness than base metal which means it has lower ductility, furthermore, the internal stresses between the FZ and base metal or the FZ and HAZ due to welding could also have promotes failure at FZ.

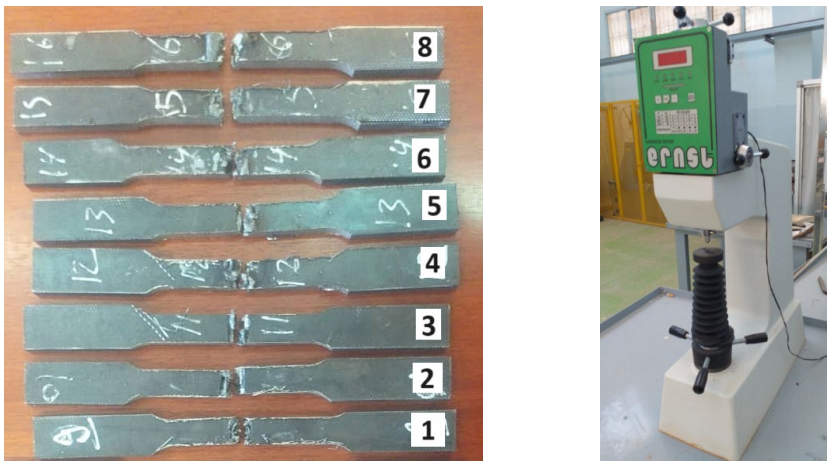

(a) (b)

Fig. 3 *Welding testing (a) Tensile test samples; (b) Rockwell hardness instrument*

Table 5 *The welding experiments with their respect response; tensile strength and hardness of welding*

Standard order	Voltage (v)	WFS (m/min)	Groove shape	Tensile strength (N/mm^2)	Heat input (kJ/mm)	Hardness (HRB)	EL%
1	20	5.9	V	305	$1.28*10^{-2}$	35.7	7
2	20	5.9	X	263	$1.28*10^{-2}$	26.7	6
3	20	10.6	V	238	$1.28*10^{-2}$	30.4	7
4	20	10.6	X	253	$1.28*10^{-2}$	24.0	6
5	27.5	5.9	V	233	$3.96*10^{-2}$	29.4	6
6	27.5	5.9	X	190	$3.96*10^{-2}$	22.4	6
7	27.5	10.6	V	192	$3.96*10^{-2}$	27.1	7
8	27.5	10.6	X	164	$3.96*10^{-2}$	23.0	4

The plots in Fig. 6 and Fig. 7 depict the main effects for signal-to-noise (S/N) ratios and means of the welding factors, respectively. In Fig. 6, the signal-to-noise ratios offer insights into the influence of welding factors by presenting their mean S/N values. These ratios gauge the impact or influence of the welding factors on achieving higher tensile strength and hardness values under varying noise conditions. Essentially, Fig. 6 provides a visual interpretation of how the welding factors contribute to desirable mechanical properties. Meanwhile, Fig. 7, representing the Means, showcases the average response values, specifically the tensile strength and hardness of the welding. This Fig. offers a comprehensive view of how each welding factor contributes to the overall outcome, providing a clear representation of the means of the response variables. Together, these plots aid in understanding the relationships between welding factors and the resulting mechanical properties in the context of the experiment.

The ranking, as outlined in Table 6, aligns with the findings in Fig. 6. Groove shape emerges as the most influential welding factor, followed by voltage, with WFS exhibiting the lowest impact on the response. In Table 7, the Means response table, voltage is observed to have a larger range of means values compared to the other welding factors, earning it the top rank. This aligns with the information presented in Fig. 7, where higher mean values are achieved at 20 V, and values drop significantly at 27.5 V. WFS and groove shape have obtained close response means values, both lower than those at voltage. Furthermore, the order of ranks in Table 6 is consistent with the absolute values of the coefficients in Table 8, further confirming the influence of each welding factor on the response variables. This comprehensive analysis aids in understanding the relative strengths of the welding factors and their impact on the experimental outcomes.

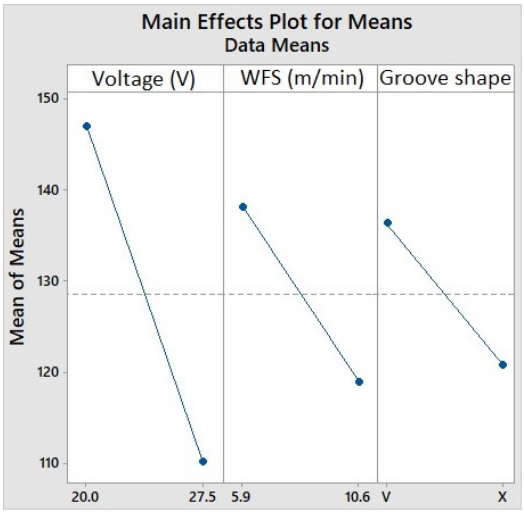

Fig. 6 *S/N ratios plot for the welding factors*

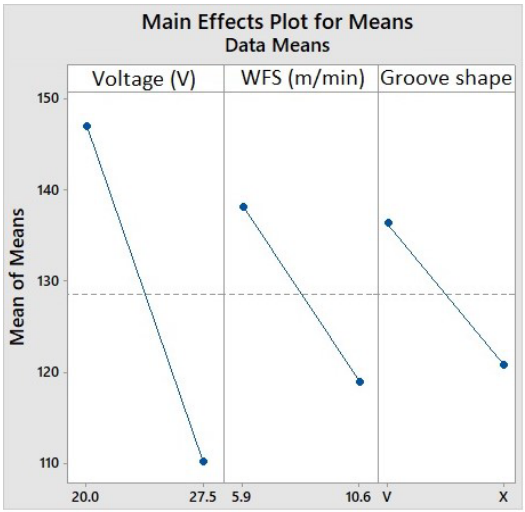

Fig. 7 *Main effect plot for means for the welding factors*

Table 6 *The S/N ratios for the welding factors and their respective ranking*

Level	Voltage (V)	WFS (m/min)	Groove shape
1	32.17	31.94	32.62
2	31.00	31.23	30.55
Delta	1.17	0.71	2.08
Rank	2	3	1

*Larger is better

Table 7 *The mean ratios for the welding factors and their respective ranking*

Level	Voltage (V)	WFS (m/min)	Groove shape
1	147.0	138.2	136.3
2	110.1	118.9	120.8
Delta	36.9	19.2	15.6
Rank	1	2	3

The estimated model coefficients and the analysis of variance for the S/N ratio related to the welding factors are detailed in Table 8 and Table 9, respectively. The tables reveal the most noteworthy findings, with the smallest P-value observed for the V-groove shape at 0.002, indicating statistical significance as it falls below the conventional significance level of 0.05. Similarly, the P-value for 20 V is also deemed significant at 0.019. Conversely, the P-value for WFS at 5.9 m/min is non-significant, registering at 0.081. This implies that the influence of WFS at this specific level on tensile strength and hardness is relatively minimal. These outcomes align with the trends observed in Fig. 6 and Table 6. The model achieves a notable fit of 89.93% on the R^2 correlation, indicating a strong correlation between the model and the observed data. The higher significance of welding parameters levels V-groove-shaped, followed by welding voltage at 20 V, emphasizes the influence of the tensile strength of welding samples. Since higher tensile results were achieved at those levels, In summary, higher welding tensile strength was achieved at the optimal welding factors, as evidenced by the S/N ratio in Fig. 6, response means values in Fig. 7, and the coefficients in Table 8, which are identified as V-groove shape, 20 V, and 5.9 m/min WFS. These factors collectively contribute to achieving desirable outcomes in terms of tensile strength and hardness in the welding process.

4. Conclusion

Mild steel plates underwent Gas Metal Arc Welding (GMAW) using a low carbon steel electrode wire. The welding process incorporated three key factors: base metal thickness, welding voltage, and Wire Feed Speed (WFS). Utilizing Taguchi's design, an analysis was conducted to assess the impact of these welding factors on the tensile strength and hardness of the welds. The findings revealed that the welding groove shape exerted the most significant influence on the results, followed by wire feed speed. In contrast, welding voltage demonstrated

the lowest impact on both tensile strength and hardness. The optimal combination of welding factors, as determined by the analysis, is V-groove shape, 20 V, and 5.9 m/min WFS. This configuration is identified as the most favorable for achieving desirable outcomes in terms of tensile strength and hardness in the welding process.

Table 8 *Coefficients for welding factors S/N ratios*

Term	Coefficient	SE Coefficient	T	P-value
Constant	31.5852	0.1536	205.670	0.000
Voltage (20 V)	0.5832	0.1536	3.797	0.019
WFS (5.9 m/min)	0.3559	0.1536	2.317	0.081
Groove shape (V)	1.0384	0.1536	6.762	0.002

Table 9 *Analysis of variance for welding factors S/N ratios*

Source	DF	Seq SS	Adj SS	Adj MS	F	P
Voltage (V)	1	2.7208	2.7208	2.7208	14.42	0.019
WFS (m/min)	1	1.0133	1.0133	1.0133	5.37	0.081
Groove shape	1	8.6269	8.6269	8.6269	45.72	0.002
Residual Error	4	0.7547	0.7547	0.1887		
Total	7	13.1156				

Acknowledgement

The author extends heartfelt gratitude to their family for the unwavering support and encouragement provided throughout the course of the study. Special thanks are extended to the Libyan Iron and Steel Company for their valuable assistance, as well as to the dedicated staff of the welding laboratory at the Saad Elkarimi Institute of Engineering Technology in Benghazi. Recognition is also given to the College of Mechanical Engineering Technology in Benghazi.

Conflict of Interest

Authors declare that there is no conflict of interests regarding the publication of the paper.

Author Contribution

The author confirms sole responsibility for the following: study conception and design, data collection, analysis and interpretation of results, and manuscript preparation.

References

[1] Su Lihong, Fei Zhenyu, Davis Bradley, Li Huijun & Bornstein Huon (2021) A review on parametric optimization of MIG welding for medium carbon steel using FEA-DOE hybrid modeling, *International Journal for scientific research & development,* 1(9), 2321-0613. https://doi.org/10.1016/j.msea.2021.142033

[2] 2 Pradipta Kumar Rout & Pankaj C. Jena (2020) Mechanical Characterization and Microstructural Study of Carbon Steel Welded Joint Made Under SMAW and GMAW Processes, *Innovative Product Design and Intelligent Manufacturing Systems*, 847-855. https://doi.org/10.1007/978-981-15-2696-1_82

[3] Rajakumar, S., Vimal Kumar, P., Kavitha, S., & Balasubramanian, V. (2020) Mechanical and Microstructural Characteristics of Conventional and Robotic Gas Metal Arc Welded Low Carbon Steel Joints: A Comparative Study, *Metallography, Microstructure, and Analysis*, 9, 337–344. https://doi.org/10.1007/s13632-020-00645-2

[4] Coşkun Hamzaçebi (2020) Taguchi Method as a Robust Design Tool. In Quality Control-Intelligent Manufacturing, Robust Design and Charts, *IntechOpen*, 1-19. https://doi.org/10.5772/intechopen.94908

[5] Tukahirwa, G., & Wandera, C. (2023). Influence of Process Parameters in Gas-Metal Arc Welding (GMAW) of Carbon Steels. In C. Sanjeev Kumar (Ed.), *Welding - Materials, Fabrication Processes, and Industry 5.0* (pp. 1–23). Intechopen. https://doi.org/10.5772/intechopen.1002730

[6] Wang, H. K., Wang, Z. H., & Wang, M. C. (2020) Using the Taguchi method for optimization of the powder metallurgy forming process for Industry 3.5, *Computers & Industrial Engineering*, *148*, 106635. https://doi.org/10.1016/j.cie.2020.106635

[7] Rajakumar, S., Vimal Kumar, P., Kavitha, S., & Balasubramanian, V. (2020) Mechanical and Microstructural Characteristics of Conventional and Robotic Gas Metal Arc Welded Low Carbon Steel Joints: A Comparative Study, *Metallography, Microstructure, and Analysis*, 9, 337-344. https://doi.org/10.1007/s13632-020-00645-2
[8] Rout, A., BBVL, D., & Biswal, B. B. (2020) Optimization of process variables of laser sensor assisted robotic GMAW process for mild steel material, *Materials and Manufacturing Processes*, 35(15), 1690-1700. https://doi.org/10.1080/10426914.2020.1784934
[9] Math, P., & Kumar, B. P. (2021) Analysis optimization and modelling of CO_2 welding process parameters in fabrication of mild steel plates, *Materials Today: Proceedings*, 45, 420-423. https://doi.org/10.1016/j.matpr.2020.12.1004
[10] Elfallah, S. S. S. (2023) Study The Influence of Welding Parameters by Taguchi's Design On the Mechanical Properties of Welded Mild Steel (S235JR), 85(4), 55–66. https://doi.org/10.11113/jurnalteknologi.v85.19653
[11] Calderón, L., Bohórquez, O., Rojas, M. A., & Pertuz, A. (2021) Experimental relationship of tensile strength and hardness of welded structural steel, *Journal of Physics: Conference Series,* 2046(1), 012065. https://doi.org/10.1088/1742-6596/2046/1/012065
[12] Assefa, A. T., Ahmed, G. M. S., Alamri, S., Edacherian, A., Jiru, M. G., Pandey, V., & Hossain, N. (2022) Experimental investigation and parametric optimization of the tungsten inert gas welding process parameters of dissimilar metals, *Materials*, 15(13), 4426. https://doi.org/10.3390/ma15134426
[13] Nallasamy Sankar, Sudersanan Malarvizhi, Visvalingam Balasubramanian (2021) Mechanical properties and microstructural characteristics of rotating arc-gas metal arc welded carbon steel joints, *Journal of the Mechanical Behavior of Materials*, 30(1), 49-58. https://doi.org/10.1515/jmbm-2021-0006
[14] Aldalur, E., Veiga, F., Suárez, A., Bilbao, J., & Lamikiz, A. (2020) High deposition wire arc additive manufacturing of mild steel: Strategies and heat input effect on microstructure and mechanical properties, *Journal of Manufacturing Processes*, *58*, 615-626. https://doi.org/10.1016/j.jmapro.2020.08.060
[15] Grzybowski, I. F., Zientarski, R. R., Buenos, A. A., & dos Santos Junior, A. A. (2022) Residual stresses in weld bead of low carbon steel plates welded by gmaw using lcr waves, *Journal of the Brazilian Society of Mechanical Sciences and Engineering*, 44(7), 290. https://doi.org/10.1007/s40430-022-03587-8
[16] Jiang, J., Peng, Z. Y., Ye, M., Wang, Y. B., Wang, X., & Bao, W. (2021) Thermal effect of welding on mechanical behavior of high-strength steel, *Journal of Materials in Civil Engineering*, 33(8), 04021186. https://doi.org/10.1061/(ASCE)MT.1943-5533.000383
[17] Nagasai, B. P., Malarvizhi, S., & Balasubramanian, V. (2022) Effect of welding processes on mechanical and metallurgical characteristics of carbon steel cylindrical components made by wire arc additive manufacturing (WAAM) technique, *CIRP Journal of Manufacturing Science and Technology*, 36, 100-116. https://doi.org/10.1016/j.cirpj.2021.11.005
[18] Standard test methods for tension testing of metallic materials (2021) Standard test methods for tension testing of metallic materials, ASTM E8-04. https://doi.org/10.1520/E0008-04
[19] World Material (2022) EN 1.0038 Steel S235JR Material Equivalent, Properties, Composition. https://www.theworldmaterial.com/1-0038-steel-s235jr-material/
[20] Yeni Ratih Pratiwi & Salnan Sabdo Wibowo (2019) The Effect of Electrode and Number of Passes on Hardness and Micro Structure of Shielded Metal Arc Welding, *IOP Conference Series: Materials Science and Engineering. IOP Publishing*, 515(1), 012072. https://doi.org/10.1088/1757-899x/515/1/012072
[21] Pawlik, J., Cieślik, J., Bembenek, M., Góral, T., Kapayeva, S., & Kapkenova, M. (2022) On the Influence of Linear Energy/Heat Input Coefficient on Hardness and Weld Bead Geometry in Chromium-Rich Stringer GMAW Coatings, *Materials*, *15*(17), 6019. https://doi.org/10.3390/ma15176019
[22] Scharf-Wildenhain, R., Haelsig, A., Hensel, J., Wandtke, K., Schroepfer, D., Kromm, A., and Kannengiesser, T. (2022) Influence of Heat Control on Properties and Residual Stresses of Additive-Welded High-Strength Steel Components, *Metals*, 12(6), 951. https://doi.org/10.3390/met12060951
[23] Lahtinen, T., Vilaça, P., Peura, P., and Mehtonen, S. (2019) MAG Welding Tests of Modern High Strength Steels with Minimum Yield Strength of 700 MPa, *Applied Sciences*, *9*(5), 1031. https://doi.org/10.3390/app9051031.
[24] Ahmed, M. M., Ataya, S., El-Sayed Seleman, M. M., Mahdy, A. M., Alsaleh, N. A., and Ahmed, E. (2020) Heat Input and Mechanical Properties Investigation of Friction Stir Welded aa5083/aa5754 and aa5083/aa7020, *Metals*, 11(1), 68. https://doi.org/10.3390/met11010068